nature plants

Supplementary information

https://doi.org/10.1038/s41477-024-01760-6

Arabidopsis floral buds are locked through stress-induced sepal tip curving

In the format provided by the authors and unedited

Arabidopsis floral buds are locked through stress-induced sepal tip curving

Duy-Chi Trinh[1,2,*], Isaty Melogno[1], Marjolaine Martin[1], Christophe Trehin[1], Richard S. Smith[3] and Olivier Hamant[1,*]

[1] Laboratoire de Reproduction et Développement des Plantes, Université de Lyon, ENS de Lyon, UCBL, INRAE, CNRS, 46 Allée d'Italie, 69364 Lyon Cedex 07, France

[2] University of Science and Technology of Hanoi. Vietnam Academy of Science and Technology (VAST), 18 Hoang Quoc Viet, Cau Giay, Ha Noi, Vietnam

[3] Department of Computational and Systems Biology, John Innes Centre, Norwich NR4 7UH, UK.

* Corresponding authors: trinh-duy.chi@usth.edu.vn, olivier.hamant@ens-lyon.fr

Inventory of Supporting information

Material and Methods

Material

All experiments were performed on Co-0 ecotype. The *vip3-1* (Salk_139885) mutant was described in (Fal et al., 2019). The *mad5, spr2-2* and *xxt1xxt2* mutants was described in [2,5,6], respectively. The plasma membrane marker line *pUBQ10::Lti6b-tdTomato* was described in[3] and the microtubule marker line *pDF1::mCitrin-MBD* was described in[4]. For all analyses on sepals, plants were grown on soil at 20°C in short-day conditions (8h light/16h dark) for 3 weeks then transferred to long-day conditions (16h light/8h dark cycle).

Table 1. Material used in this study

Material	SOURCE
Experimental models: Organisms/strains	
Arabidopsis Col-0	Widely available
mad5	[2]
spr2-2	[5]
xxt1 xxt2	[6]
vip3-1	[7,1]
pUBQ10::Lti6b-tdTomato	[3]
pDF1::mCitrin-MBD	[4]
*pWOX1::sYFP2-PHS1*ΔP	This study
Recombinant DNA	
pDONR-Zeo/AtPHS1_85-700 (PHS1dP)	[8]
*pB7m34GW pWOX1::sYFP2-PHS1*ΔP	This study
Software and algorithms	
MorphoGraphX	[9]
MorphoMechanX	[10]
Kappa (κ) plug-in for ImageJ	[11]

Construction of transgenic cassettes and plant transformation

pWOX1::sYFP2-PHS1deltaP was created from intermediate vectors using the Gateway three fragment cloning system according to the manual. The WOX1 promoter was a gift from Professor Feng Zhao (School of Ecology and Environment, Northwestern Polytechnical University, Xi'an, Shaanxi, China). Basically, a DNA fragment of 1995bp upstream of the WOX1 full length coding sequence, plus 181bp in the WOX1 coding sequence was cloned into pDONR P4-P1R vector. The fluorophore sYFP2 was in pDONR-221 vector. DNA sequence of the truncated version of PHS1 (PHS1ΔP, lacking the phosphatase catalytic domain and the putative kinase-interacting motif)[8] was in pDONR-Zeo plasmid and was a gift from Dr. Takashi Hashimoto (Division of Biological Science,

Nara Institute of Science and Technology, Ikoma, Nara 630-0192, Japan); *PHS1ΔP* was then cloned into pDONR P2R-P3. These components were then combined into a pB7m34GW vector (basta resistant) to create *pWOX1::sYFP2-PHS1deltaP*. The floral dip method was used to transform Arabidopsis plants with Agrobacterium tumefaciens[12]. The successfully transformed plants were selected based on herbicide (basta) resistance and phenotype. More than 10 independent transformation events were obtained, all showing similar seedling and inflorescence phenotype (Figure S1).

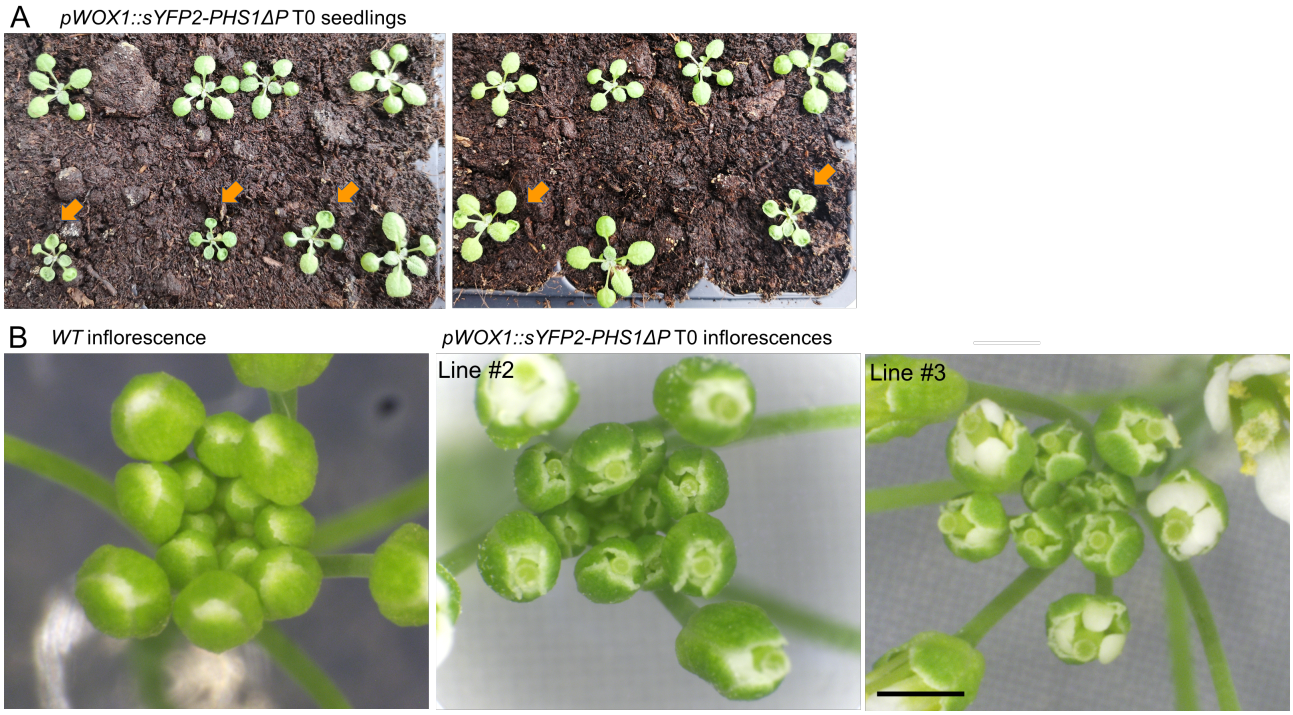

Figure S1. *pWOX1::sYFP2-PHS1ΔP* seedlings and flower phenotype

(A) Seedlings of independent transformation events (T0). They show similar phenotype, such as sunken patches of tissues on true leaves. (B) More images of flower phenotype of different lines showing similar phenotype.

Sample imaging

Sepals were imaged using a Leica binocular. The flower buds were placed so that the abaxial sepal is on its side to reveal its longitudinal curvature. For confocal imaging to track sepal growth or verify gene expression pattern, the Leica SP8 confocal microscope equipped with a resonant scanner and a 20x water dipping objective was used. Inflorescence samples were prepared as described in [13]. For sYFP2 excitation, we used the 514 nm laser, and collected wavelength in the 520-540 nm range; for mCitrine: 514nm, 520-540 nm; for Propidium Iodide (PI): 514 nm, 610-650 nm; for tdTomato: 552 nm, 570-605 nm.

Measuring sepal curvature and sepal curving

The longitudinal curvature *k* of a sepal can be measured as $k = 1/R$, with *R* being the radius of a circle best fit the sepal curve. To measure *k*, we used the Kappa plugin in ImageJ [11]. The plugin produces several curve descriptors, including curve length and curvature.

However, as sepals keep growing, the radii of the corresponding circles grow as well, so that sepal curvatures decreases. Measuring the curvature $k = 1/R$ may not the clearest way to discriminate between different situations.

To test different methods to discriminate between several scenarios of changes in sepal curving, we created four set of shapes (four scenarios): in scenario #1, the shapes are simply homothetic deformations from the original shape; in scenario #2, axial growth is larger than lateral growth, the shape becomes more curved; in scenario #3, axial growth is lower than lateral growth, the shape becomes flatter; and scenario #4 mixes periods where axial and lateral growth dominate alternatively (Figure S1D).

The curvature *k* of these shapes was first measured. As illustrated in Figure S1E, the dynamics in the curvature of the four scenarios are very similar, despite the opposite changes in curving, for example, between scenario #2 and scenario #3. It confirms that the curvature $k = 1/R$ is not the best parameter to describe curving.

We then explored the use of the *curving score*, defined as the aspect ratio width/length of the box bounding the shape contour as viewed from the side. To do so, we extracted the contour of the shape manually in Fiji (add as ROI), then a tilted bounding box of the curve was identified using the function: Edit > Selection > Fit rectangle (add as ROI). Then the curve length and the box parameters were measured, which produce the box's width and length. The aspect ratio width/length of the bounding box was used as a proxy for curving. We found that the curving score can discriminate the four scenarios (Figure S2F).

We then tested the use of the curvature $k = 1/R$ and the curving score to a real dataset of sepals growing over a seven-day period (exemplified in Figure 2D) to see if these parameters can be used to describe changes in sepal curving. First, we measured the curvature $k = 1/R$ of these sepals (Figure S2A, upper panel), and found that their curvature reduces over time (Figure S2B and S2E), similar to what we found for the artificial shapes. To reduce the influence of growth over the curvature values, we normalized the length of the sepals at each time point so that they always have the same length (500µm, as an arbitrary value; Figure S2A, bottom panel). We call these shapes "normalized sepals". As expected, measuring curvature of these normalized sepals provided different curvature dynamics than non-normalized sepals (Figure S2C). These dynamics fit well with the observed changes in sepal curving over time. Finally, we calculated the curving score of the normal sepals and found similar dynamics compared to the curvature values for normalized sepals (Figure S2D). Because the curving

score (aspect ratio width/length of the box bounding the sepal contour) is dimensionless and more intuitive than the curvature $k = 1/R$, we used it to describe changes in sepal curving throughout the paper.

Growth analyses

The MorphoGraphX (MGX) 3D image analysis software was used for cell segmentation, cell growth calculation and growth pattern visualization, following the official manual [14].

Osmotic treatment

To assess relative cell wall stiffness between regions of the sepal, we treated floral buds with a hyperosmotic solution as described in [15]. The flowers were at stage 6 where the abaxial sepal already encloses the bud, but yet to experience a sharp increase in sepal curving [16]. The cuticular ridges were not detected at this stage. Basically, the sepal was first stained with 0.1% solution of propidium iodide in water for 15min and then treated with salt solution (NaCl 0.4M) for 30min. In these conditions, cells lose water via osmosis and shrink in size. The confocal images of the sepal before and after treatment was taken. The images were then segmented in MorphoGraphX, and changes in surface area of cells due to the treatment were calculated (shrinkage in percentage). A large shrinkage indicates a softer cell wall, and vice versa. Small cells were grouped into larger regions when the cell wall signals were illegible.

Computational model

The MorphoMechanX (www.MorphoMechanX.org) modeling framework was used for the FEM simulation as in [10]. In brief, growth was implemented by increasing the size of the reference configuration of the elements, with independent control of growth parallel or perpendicular to a growth axis. The rates of growth and the growth direction were specified manually based on qualitative assessment of live imaging data. After each growth step, the mechanical equilibrium was found, and residual stresses were released. Any wedges above a threshold volume were subdivided, and values for growth parameters were reassigned.

Quantification and statistical analysis

Data plotting and statistical analyses were performed in Microsoft Excel and in R.

SUPPLEMENTARY REFERENCES

1. Trinh, D.-C. *et al.* Increased gene expression variability hinders the formation of regional mechanical conflicts leading to reduced organ shape robustness. *Proc. Natl. Acad. Sci. U. S. A.* **120**, e2302441120 (2023).
2. Brodersen, P. *et al.* Widespread Translational Inhibition by Plant miRNAs and siRNAs. *Science* **320**, 1185–1190 (2008).
3. Shapiro, B. E., Tobin, C., Mjolsness, E. & Meyerowitz, E. M. Analysis of cell division patterns in the Arabidopsis shoot apical meristem. *Proc. Natl. Acad. Sci. U. S. A.* **112**, 4815–4820 (2015).
4. Stanislas, T. *et al.* A phosphoinositide map at the shoot apical meristem in Arabidopsis thaliana. *BMC Biol.* **16**, 20 (2018).
5. Hervieux, N. *et al.* A Mechanical Feedback Restricts Sepal Growth and Shape in Arabidopsis. *Curr. Biol. CB* (2016) doi:10.1016/j.cub.2016.03.004.
6. Cavalier, D. M. *et al.* Disrupting Two *Arabidopsis thaliana* Xylosyltransferase Genes Results in Plants Deficient in Xyloglucan, a Major Primary Cell Wall Component. *Plant Cell* **20**, 1519–1537 (2008).
7. Fal, K. *et al.* Tissue folding at the organ-meristem boundary results in nuclear compression and chromatin compaction. *Proc. Natl. Acad. Sci. U. S. A.* **118**, (2021).
8. Fujita, S. *et al.* An atypical tubulin kinase mediates stress-induced microtubule depolymerization in Arabidopsis. *Curr. Biol. CB* **23**, 1969–1978 (2013).
9. de Reuille, P. B. *et al.* MorphoGraphX: A platform for quantifying morphogenesis in 4D. *eLife* **4**, 1–20 (2015).
10. Harline, K. *et al. Dynamic Growth Re-Orientation Orchestrates Flatness in the Arabidopsis Leaf*. http://biorxiv.org/lookup/doi/10.1101/2022.11.01.514736 (2022) doi:10.1101/2022.11.01.514736.
11. Mary, H. & Brouhard, G. J. Kappa (κ): Analysis of Curvature in Biological Image Data using B-splines. *bioRxiv* 1–14 (2019).
12. Clough, S. J. & Bent, A. F. Floral dip: a simplified method forAgrobacterium-mediated transformation ofArabidopsis thaliana: Floral dip transformation of Arabidopsis. *Plant J.* **16**, 735–743 (1998).
13. Stanislas, T., Hamant, O. & Traas, J. In-vivo analysis of morphogenesis in plants. in vol. 139 203–223 (2017).
14. Strauss, S. *et al.* Using positional information to provide context for biological image analysis with MorphoGraphX 2.0. *eLife* **11**, e72601 (2022).
15. Sapala, A. & Smith, R. S. Osmotic Treatment for Quantifying Cell Wall Elasticity in the Sepal of Arabidopsis thaliana. in *Plant Stem Cells* (eds. Naseem, M. & Dandekar, T.) vol. 2094 101–112 (Springer US, New York, NY, 2020).
16. Smyth, D. R., Bowman, J. L. & Meyerowitz, E. M. Early flower development in Arabidopsis. *Plant Cell* **2**, 755–767 (1990).